



HAL
open science

Improving Raman velocimetry of laser-cooled cesium atoms by spin-polarization

Julien Chabé, Hans Lignier, Pascal Szriftgiser, Jean Claude Garreau

► **To cite this version:**

Julien Chabé, Hans Lignier, Pascal Szriftgiser, Jean Claude Garreau. Improving Raman velocimetry of laser-cooled cesium atoms by spin-polarization. *Optics Communications*, 2007, 274 (1), pp.254-259. 10.1016/j.optcom.2007.02.008 . hal-00021689v2

HAL Id: hal-00021689

<https://hal.science/hal-00021689v2>

Submitted on 3 Feb 2007

HAL is a multi-disciplinary open access archive for the deposit and dissemination of scientific research documents, whether they are published or not. The documents may come from teaching and research institutions in France or abroad, or from public or private research centers.

L'archive ouverte pluridisciplinaire **HAL**, est destinée au dépôt et à la diffusion de documents scientifiques de niveau recherche, publiés ou non, émanant des établissements d'enseignement et de recherche français ou étrangers, des laboratoires publics ou privés.

Improving Raman velocimetry of laser-cooled cesium atoms by spin-polarization

Julien Chabé, Hans Lignier,¹ Pascal Szriftgiser,
Jean Claude Garreau

*Laboratoire de Physique des Lasers, Atomes et Molécules, UMR CNRS 8523,
Centre d'Études et de Recherches Laser et Applications, Université des Sciences et
Technologies de Lille, F-59655 Villeneuve d'Ascq Cedex, France.*²

Abstract

We study the performances of Raman velocimetry applied to laser-cooled, spin-polarized, cesium atoms. Atoms are optically pumped into the $F = 4$, $m_4 = 0$ ground-state Zeeman sublevel, which is insensitive to magnetic perturbations. High resolution Raman stimulated spectroscopy is shown to produce Fourier-limited lines, allowing, in realistic experimental conditions, atomic velocity selection to one-fiftieth of a recoil velocity.

Key words: Raman velocimetry, spin polarization, laser-cooled atoms

PACS: 42.50.Vk, 32.80.Pj, 32.60.+i

1 Introduction

Raman stimulated spectroscopy has been one of the most fertile techniques used for manipulating laser-cooled atoms. It has been used for atomic velocity selection (1), sub-recoil laser cooling (2; 3) and quantum state preparation and detection (4; 5), with applications in as different fields as quantum chaos (6; 7), quantum dynamics in optical lattices (8; 9; 10), quantum information processing (11), and high-precision metrology of fundamental constants (12; 13; 14). Being a *stimulated* two-photon transition between two ground-state hyperfine sublevels, the width of the Raman line is, in principle, limited only by the duration of interaction between the atom and the light (the Fourier limit), as no natural widths are involved in the process. These sharp transitions

¹ Present address: Dipartimento di Fisica “E. Fermi”, Università di Pisa, Pisa, Italy

² <http://www.phlam.univ-lille1.fr/atfr/cq>

can thus be used to select a very thin velocity class. A laser radiation of wavelength λ_L produces optical potentials with a typical well width of the order of $\lambda_L/2$ (e.g. in a standing wave), whereas the so-called *recoil velocity* $v_r = \hbar k_L/M$ (with $k_L = 2\pi/\lambda_L$ and M the mass of the atom) corresponds to a de Broglie wavelength $\lambda_{dB} = \lambda_L$. One thus sees that the deep quantum regime $\lambda_{dB} \gg \lambda_L/2$ implies very sharp, “sub-recoil”, velocity distributions with $\langle v^2 \rangle^{1/2} \ll v_r$, which cannot be obtained in a simple magneto-optical trap.

For the alkaline atoms, the ground state presents hyperfine Zeeman sublevels, so that the Zeeman effect and light shifts inhomogeneously broaden the Raman transition. In order to obtain sharper lines one must pump the atoms into a particular sublevel, avoiding inhomogeneous broadening. In this respect, the $m_F = 0$ Zeeman sublevel³ is particularly interesting, as this level is not affected by the first order Zeeman effect, and the second order effect is negligible for the low magnetic fields we are considering here⁴.

Atom spin polarization has been used in many recent experiments in various fields. In metrology, it was used in building frequency standards (15), measuring the ratio h/M in cesium (12) and rubidium (13), and in a recent determination of the fine structure constant (14). It has also played an important role in optical dipole traps and sideband cooling (16; 17; 18). None of these works, however, concentrate in the polarization process itself. The aim of the present work is thus to study in greater detail the polarization process in the context of Raman velocimetry of cold atoms. We describe a setup allowing optical pumping of laser-cooled cesium atoms into the $F = 4$, $m_4 = 0$ ground-state hyperfine sublevel, concentrating on the improvement of the sensitivity of the Raman velocimetry (RV) technique. This allows us, moreover, to measure and minimize the heating induced in the atoms by the polarization process itself. We achieve a degree of polarization of $\sim 75\%$ of the atoms in the $m_4 = 0$ sublevel with an increase of the *rms* velocity limited to 20%. The observed Raman transition full width at half maximum (FWHM) is 160 Hz, which corresponds to a velocity resolution of $v_r/50$ (or 70 $\mu\text{m/s}$, the best reported velocity resolution to our knowledge), to be compared to the $v_r/2$ resolution of the compensated-magnetic-field line we observed in the same experimental setup (19) with unpolarized atoms. We show that the Raman line resolution (in the velocity-independent case) is Fourier-limited, i.e. the width of the line is comparable to the inverse of the duration of the Raman pulse. In this sense, we can say that we approached the RV ultimate limit.

³ Throughout this paper, except otherwise indicated, we use the following convention to note Zeeman sublevels: ground state sublevels are noted F, m_F and excited-state sublevels are noted $F', m_{F'}$.

⁴ The order of magnitude of the *broadening* induced by the second order Zeeman effect in our setup is 1 mHz.

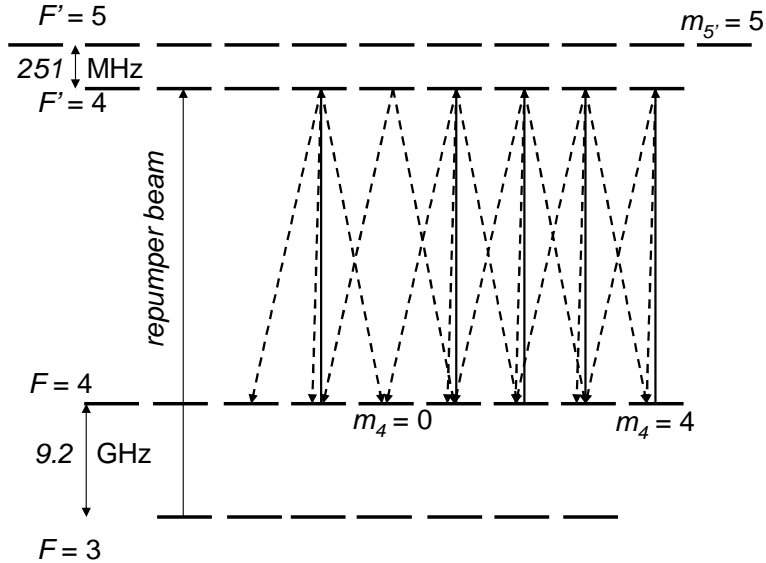


Figure 1. Pumping atoms with a π -polarized radiation on a $F \rightarrow F'$ transition polarizes the atoms in the magnetic field-insensitive $m_4 = 0$ Zeeman sublevel. Laser-induced transitions are represented by solid arrows, spontaneous-emission transitions by dashed arrows. In order to keep the figure readable, we did not represent all possible transitions.

2 Experimental setup

In this section, we briefly discuss basic aspects of atom spin polarization. We consider specifically the case of the cesium atom, although most of our conclusions can be easily extended to other alkalis. Atomic spin polarization is performed in the presence of a *bias magnetic field*, which defines a fixed quantization axis for all atoms.

The polarization technique we use, schematically presented in Fig. 1, is based on the fact that the Clebsch-Gordan coefficient coupling the ground state sublevel $F, m_F = 0$ to the excited sublevel $F', m_{F'} = 0$ vanishes. This means, for cesium, that if one optically pumps the atom with *linearly polarized light* on the $F = 4 \rightarrow F' = 4$ transition, the $m_4 = 0$ level is a dark state, in which atoms are trapped. Because they are in a dark state, they are not submitted to spontaneous emission heating due to fluorescence cycles. The transition is however not closed, as the atoms can spontaneously decay from the excited $F' = 4$ level to the $F = 3$ level, so that one must use a repumper laser beam coupling the levels $F = 3$ and $F' = 4$, which brings those atoms back into the polarizing cycle.

Our experimental setup (fig. 2) consists of a standard magneto-optical trap (MOT), a polarizing beam, a repumper beam and a stimulated Raman spectroscopy setup. This setup can be used in two different configurations. If the Raman beams are copropagating, one can measure individual Zeeman sublevel

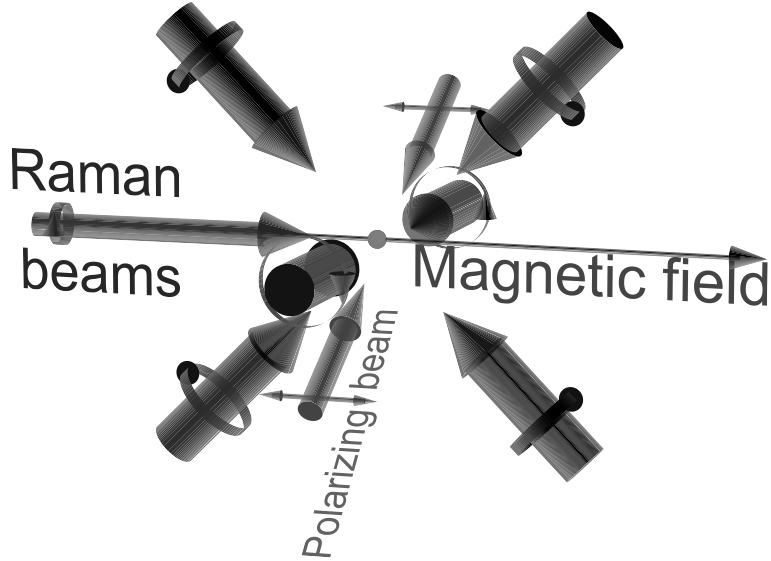


Figure 2. Experimental setup. The atomic cloud is at the center. Three back-reflected beams (thick arrows) provide magneto-optical trapping and cooling, two σ^+ Raman beams (thin arrows) (displayed here in the copropagating configuration) induce Raman transitions. The back-reflected polarizing beam (thinner arrows) is linearly polarized along the bias magnetic field. The Raman beams are horizontal and aligned with the bias magnetic field, while the PB is orthogonal to it, making a 45° angle with respect to the horizontal.

populations, as the dependence in the atomic velocity due to Doppler effect cancels out in such case. If the beams are counterpropagating, the Doppler effect makes the transition probability dependent on the velocity, and the setup can be used to measure velocity class populations, and thus to reconstruct velocity distributions. Our laser-cooling sequence includes a 25 ms-long Sisyphus-molasses phase with a large detuning (-6Γ) and small intensity (1% of the saturation intensity) which allows us to achieve a final temperature around $3 \mu\text{K}$, close to the Sisyphus limit temperature (20). The polarizing beam (PB), whose polarization axis is parallel to the bias magnetic field, is extracted from the same diode laser that produces the MOT beams. An independent acousto-optical modulator controls its frequency. After interacting with the atom cloud, the PB is reflected back on the cloud by a mirror, preventing the atoms to be pushed out of the axis of the setup by the radiation pressure. The typical incident power on the atom cloud is $2.5 \mu\text{W}$. More details on our experimental setup can be found in previous publications (21; 19).

Atoms issued from the MOT setup are mostly in the $F = 4$ ground-state hyperfine level. The Raman-resonant atoms are transferred by a Raman pulse to the $F = 3$ level and the atoms remaining in the $F = 4$ level are pushed out of the interaction region by a resonant pushing-beam pulse. Atoms in the $F = 3$ level are then optically repumped to the $F = 4$ level where they are excited by (frequency-modulated) resonant light and their fluorescence is

optically detected with a lock-in amplifier.

The magnetic field fluctuations are reduced in our setup by an active compensation scheme: small coils with the axis oriented along the three orthogonal directions and located at opposite corners of the cesium-vapor cell measure the magnetic field fluctuations, which are electronically interpolated to deduce a value at the *center* of the cell. This error signal is used to generate currents sent through 3 mutually orthogonal Helmholtz coil pairs that generate a compensating field. A constant bias current can also be applied to the compensating coils in order to correct the DC component of the magnetic field⁵ (we verified that this component remains stable to better than 1% over periods of time of one hour). This scheme allows thus a reduction of the magnetic field fluctuations even if one wants to keep a constant, non zero, bias field. We measured a residual magnetic field *rms* fluctuation of 300 μG (19).

In the present work we use σ^+ -polarized Raman beams (11), so that a given Raman transition involves only two Zeeman sublevels $m_F \rightarrow m_F + 1 \rightarrow m_F$, and the intensity of each line in the Raman spectrum measures the individual sublevel populations.

3 Polarizing the atoms

In order to measure the polarization, we perform Raman stimulated spectroscopy with *copropagating* beams, for which the transition is insensitive to the atomic velocity. The bias magnetic field is adjusted so that Raman lines are clearly separated. Fig. 3 compares the Raman spectra obtained without (a) and with (b) polarization. In presence of the PB, 75% of the atoms have been pumped into the $m_4 = 0$ sublevel. The fact that not all the atoms are in the dark state can be attributed to experimental imperfections in defining the polarization of the PB beam, due to its transmission through the MOT cell walls at an angle that is not exactly 90° , and to a residual misalignment between the PB polarization and the bias magnetic field, whose direction varies a little bit across the atom cloud. Polarizations higher than 95% were reported in the literature, (16; 22), but optimizing our setup to such level would imply an overall redesigning, which is not worth a gain of $\sim 20\%$ in the atom number. By comparing the total area in all lines in the two spectra, we deduce that about 20% of the atoms were lost in the polarization process, which can be attributed essentially to the atom cloud free fall due to gravity.

In Fig. 4(a) we show the line obtained with unpolarized atoms, bias magnetic

⁵ In order to adjust the bias current, we minimize the width of the Raman line in the copropagating configuration.

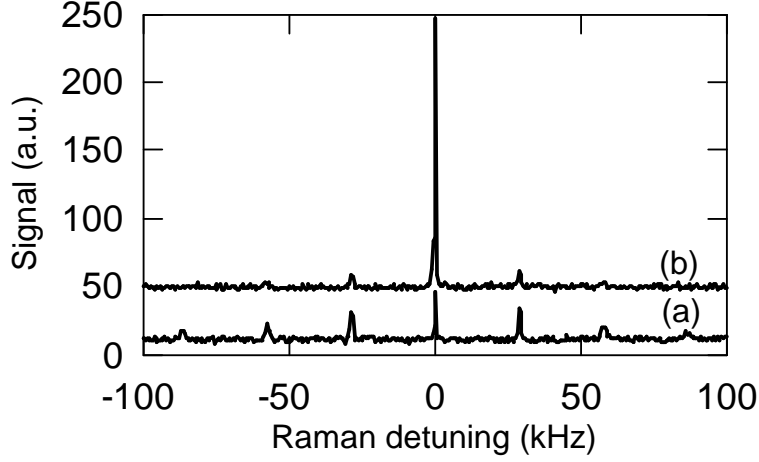


Figure 3. Copropagating-beam Raman spectra. (a) No polarizing beam applied. (b) Polarizing beam applied (this plot was vertically shifted in order to easy comparison); 75 % of the atoms are in the $m_4 = 0$ Zeeman sublevel. The power of the PB is $2.5 \mu\text{W}$ and its detuning -0.5Γ .

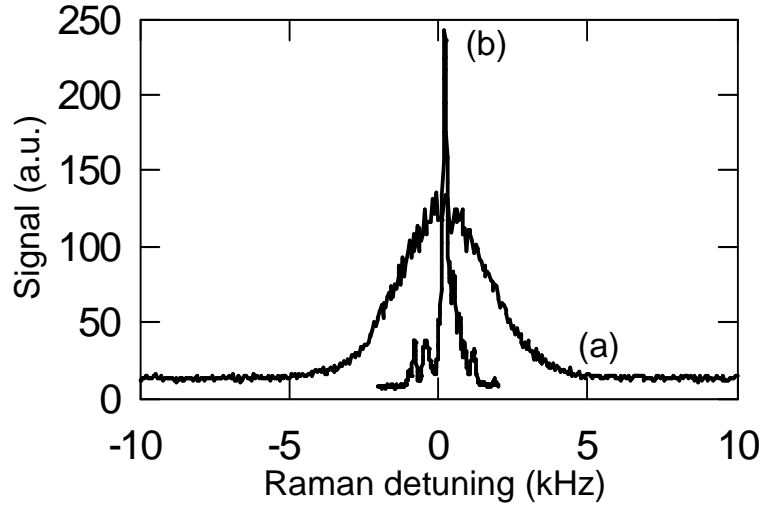


Figure 4. Comparison between copropagating-beam Raman spectra: (a) the unpolarized line obtained with no bias field (3.5 kHz FWHM) and the active compensation of the magnetic field on, and (b) the polarized $m_4 = 0$ line. The FWHM of the polarized line is 160 Hz, which implies a velocity resolution of $v_r/50$.

field tuned to zero, and the active compensation of field fluctuations on. This line includes contributions from all Zeeman sublevels, and its width can be attributed to inhomogeneous broadening of the various components due to light-shift and residual magnetic-field fluctuations (19). This line is compared to the single polarized $m_4 = 0$ line. The improvement factor in the FWHM is 22. The measured FWHM of the polarized line is 160 Hz, which, when multiplied by the Raman pulse duration (7 ms) gives 1.12: we are thus very close

Δ_{PB}	τ	P	FWHM	v_{rms}
(Γ)	(ms)	(μ W)	(kHz)	(v_r)
-1.0	0.53	2.41	98.6	5.2
-0.5	0.32	2.34	91.3	4.8
0.0	0.65	2.36	99.6	5.2
No PB	–	–	75.3	4.0

Table 1

Heating induced by the polarization process. Parameters are the detuning Δ_{PB} and the power P of the polarizing beam and τ the total duration of the polarization process (the duration is chosen so that 50% of the atoms are pumped into the $m_4 = 0$ level).

to the Fourier limit. The structures in the pedestal of the polarized line are due to weak $m_4 = 0 \rightarrow m_3 = \pm 1$ and $m_4 = \pm 1 \rightarrow m_3 = 0$ transitions due to the fact that the Raman beams wavevectors are not perfectly aligned with the bias magnetic field. In the counterpropagating case, the Doppler broadening prevents a direct measure of the resolution. However, as the perturbing effects are identical as in the copropagating case, it is rather safe to assume that the resolution is the same also in both cases.

The fluorescence cycles performed by the atom during the polarization process inevitably induce spontaneous-emission heating. In order to evaluate this heating effect, we compared the lines obtained in the *counterpropagating* Raman beam configuration with and without polarization. The observed width of 160 Hz in the polarized case corresponds, when extrapolated to the counterpropagating configuration, to a velocity resolution of $\sim 0.02v_r$, to be compared to $\sim 0.4v_r$ in the unpolarized case. Table 1 displays the parameters used and the observed linewidths. A back-reflected PB produces a minimum of heating for a detuning of -0.5Γ , corresponding to the minimum temperature of the Doppler cooling. We then observe an increase in the *rms* velocity of only 20%, from 4.0 to 4.8 v_r . We can roughly interpret this heating effect by calculating the number of fluorescence cycles necessary to bring an atom from a Zeeman substate m_F to the substate $m_F = 0$ and averaging over both m_F and over the random direction of the spontaneously-emitted photons. We obtain a value for the increase in the *rms* velocity of 1.1 v_r , which matches well with the experimental values shown in Table 1.

Fig. 5 compares the counterpropagating-beam spectra obtained with and without the application of the PB. They are very well fitted by Gaussians, and can be considered as directly proportional to the velocity distribution. The ratio of the surfaces of the two distributions is $\sim 11\%$ which constitutes a rather acceptable loss. We also observed a decrease of a factor 1.8 in the signal to noise ratio in the polarized case. This is probably due to the fact that the

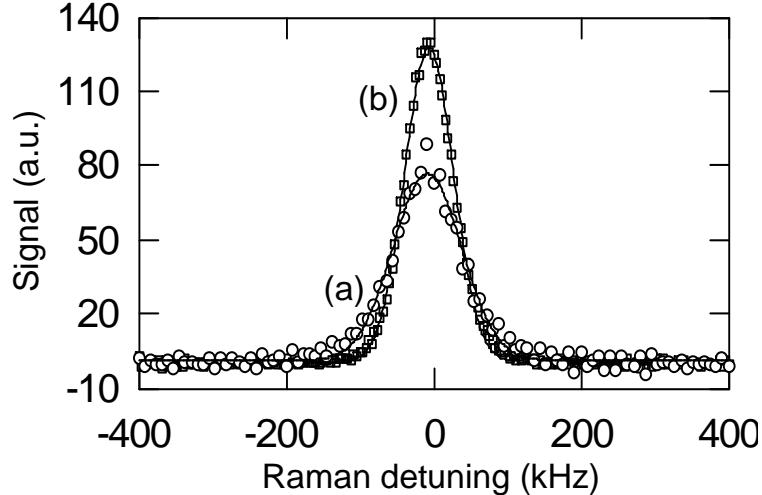


Figure 5. Counterpropagating-beam, velocity-sensitive Raman spectra. (a) Spectrum obtained with atomic polarization on the $m_4 = 0$ line (empty circles); (b) spectrum obtained with active compensation of the magnetic field (empty squares). Both lines are well fitted by Gaussians, from which one deduces *rms* velocities of, resp., 4.8 and $4.0 v_r$, (4.6 and $3.2 \mu\text{K}$). For comparison, the recoil velocity corresponds to 8.27 kHz of Raman detuning.

number of atoms present in the cloud has larger fluctuations because of the polarization process itself, as compared to the fluctuations observed in the absence of polarization. That is, the polarization both reduces the number of atoms and increases its fluctuations, thus degrading the signal to noise ratio more strongly than the observed loss in the atom number.

Finally, we have modeled the dynamics of the polarization process, and quantified the main stray effect, namely the polarization defect of the PB. Fig. 6 shows a comparison of the experimentally observed level populations and the evolution predicted by a rate-equation model described in appendix A. The simulation fits very well the experimental results, except for the population of the $m_4 = 1$ level with $\Delta_{PB} = 0$, where one observes a systematic shift, probably due to the fact that these small values are close to the limit detection level. We deduce a rather small depolarization value of $\alpha = 0.013$ [see Eq. (A.4)] , which shows that the polarization process is very sensitive to this effect.

4 Conclusion

We evidenced the ability of the polarization technique to produce very sharp Raman lines, allowing high-resolution Raman velocimetry of laser-cooled atoms. Our results imply a velocity resolution of $70 \mu\text{m/s}$, or $v_r/50$, which can be compared to $v_r/18$ reported in (8), $v_r/17$ in (22) (both with cesium) and $290 \mu\text{m/s}$, or $v_r/100$, in (1) (for sodium). The present work thus corresponds to

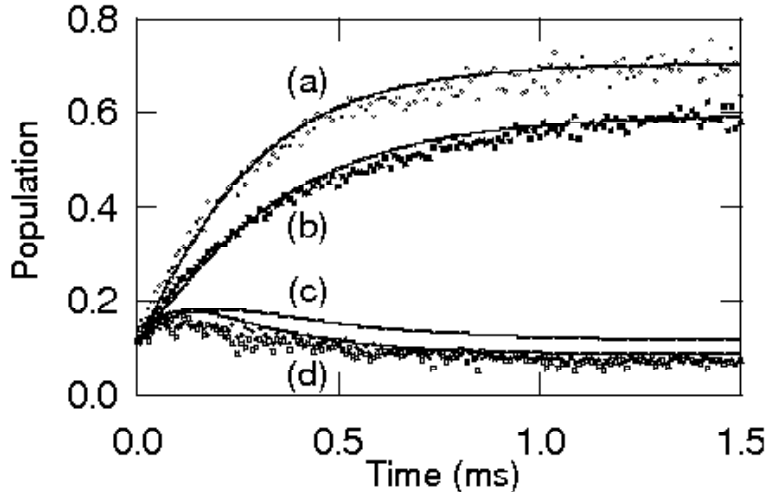


Figure 6. Dynamics of the polarization process. (a) Population of the $m_4 = 0$ level with $\Delta_{PB} = -0.5\Gamma$, (solid lines are fits of the experimental data by numerical simulation curves); (b) Population of the $m_4 = 0$ level with $\Delta_{PB} = 0$; (c) Population of the $m_4 = 1$ level with $\Delta_{PB} = 0$; (d) Population of the $m_4 = 1$ level with $\Delta_{PB} = -0.5\Gamma$. Parameters are $I_{PB}/I_s = 0.019$, $I_{repumper}/I_s = 0.023$, $\alpha = 0.013$ [cf. Eq. (A.4)].

the best observed *velocity* resolution. Such a resolution implies a de Broglie wavelength of $50\lambda_L$, which potentially generates coherent atomic wavefunctions extending up to 100 wells of a standing wave. The technique is thus highly useful in manipulating the external degrees of freedom of atoms in the frame of experiments on quantum dynamics.

Acknowledgements

Laboratoire de Physique des Lasers, Atomes et Molécules (PhLAM) is Unité Mixte de Recherche UMR 8523 du CNRS et de l'Université des Sciences et Technologies de Lille. Centre d'Études et de Recherches Laser et Applications (CERLA) is supported by Ministère de la Recherche, Région Nord-Pas de Calais and Fonds Européen de Développement Économique des Régions (FEDER).

A Model

In order to understand the dynamics of the polarizing process dynamics, we performed, as in refs. (23; 24), numerical simulations based on a rate-equation approach taking into account the effect of the PB and of the repumper. We use in the present Appendix a slightly different notation: we identify a

given sublevel by three labels: $s = \{g, e\}$ characterizing fine-structure state, $F = \{3, 4, 5\}$ for the hyperfine sublevel and $m_F = \{-F \dots F\}$ for the Zeeman sublevel. The general form of these equations is then

$$\begin{aligned} \frac{dN_{s,F,m_F}}{dt} = & \sum_{s_1,F_1,m_1} W_{s_1,F_1,m_1 \rightarrow s,F,m_F} N_{s_1,F_1,m_1} - \\ & \sum_{s_1,F_1,m_1} W_{s,F,m_F \rightarrow s_1,F_1,m_1} N_{s,F,m} + \\ & \delta_{s,g} \sum_{s_1,F_1,m_1} \Gamma a_{e,F_1,m_1 \rightarrow g,F,m_F} N_{g,F_1,m_1} - \\ & \delta_{s,e} \Gamma N_{e,F,m}. \end{aligned} \quad (\text{A.1})$$

where N_{s,F,m_F} is the population of the sublevel $\{s, F, m_F\}$, $W_{s,F,m_F \rightarrow s_1,F_1,m_1}$ is the stimulated transition rate between levels $\{s, F, m_F\}$ and $\{s_1, F_1, m_1\}$, and $a_{e,F_1,m_1 \rightarrow g,F,m_F}$ is the spontaneous emission branching ratio connecting the sublevels $\{e, F_1, m_1\}$ and $\{g, F, m_F\}$. The absorption and stimulated emission rates $W_{s,F,m_F \rightarrow s_1,F_1,m_1}$ are related to the spontaneous emission rates $a_{e,F_1,m_1 \rightarrow g,F,m_F}$ by the following relation:

$$W_{s,F,m_F \rightarrow s_1,F_1,m_1} = \frac{3}{2} \frac{\lambda_L^3}{\pi h c} \frac{I}{\Delta_L} \chi_{F \rightarrow F_1} a_{e,F_1,m_1 \rightarrow g,F,m_F} \Gamma \epsilon_{m_F - m_1}^2 \quad (\text{A.2})$$

where $\lambda_L = 852$ nm is the laser wavelength, I the laser intensity expressed in $\text{W} \cdot \text{m}^{-2}$ and $\Delta_L \sim 2\pi \times 1$ MHz the laser linewidth, and

$$\chi_{F \rightarrow F_1} \equiv \mu(\mu + 1) \frac{\Delta_{F \rightarrow F_1}^2 + (\mu - 1)^2}{(\Delta_{F \rightarrow F_1}^2 + \mu^2 - 1)^2 + 4\Delta_{F \rightarrow F_1}^2} \quad (\text{A.3})$$

is the relative probability of exciting a neighboring transition with $\mu = \Delta_L/\Gamma$ and $\Delta_{F \rightarrow F_1} = 2(\omega_{F \rightarrow F_1} - \omega_L)/\Gamma$ the position of the atomic linewidth from the laser line. The branching ratios $a_{e,F_1,m_1 \rightarrow g,F,m_F}$ can be found in (23)⁶.

As we indicated in Sec. 3, the polarization of the PB is contaminated by σ^+ and σ^- components. This is taken into account in our simulation by writing its polarization as

$$\varepsilon = \frac{\epsilon_0 + \alpha\epsilon_+ + \alpha\epsilon_-}{\sqrt{1 + 2\alpha^2}} \quad (\text{A.4})$$

⁶ Applying Eq. (A.1) to all transitions produces a set of 43 coupled equations. We noted however that the ratio between different values of $\chi_{F \rightarrow F_1}$ can be as large as 10^4 ; some transitions can in practice be neglected, and one obtains very good results with only 23 equations :-).

α being an adjustable parameter representing the depolarization of the PB. The coupled rate equations are numerically solved using a standard 4th order Runge-Kutta integration method with the initial condition that all atoms are in the $F = 4$ ground-state level and that all of its sublevels are equally populated.

References

- [1] M. Kasevich, D. S. Weiss, E. Riis, K. Moler, S. Kasapi, S. Chu, Atomic velocity selection using stimulated Raman transitions, *Phys. Rev. Lett.* 66 (18) (1991) 2297–2300.
- [2] M. Kasevich, S. Chu, Laser cooling below a photon recoil with three-level atoms, *Phys. Rev. Lett.* 69 (12) (1992) 1741–1744.
- [3] V. Boyer, L. J. Lising, S. L. Rolston, W. D. Phillips, Deeply subrecoil two-dimensional Raman cooling, *Phys. Rev. A* 70 (4) (2004) 043405.
- [4] V. Vuletic, C. Chin, A. J. Kerman, S. Chu, Degenerate Raman sideband cooling of trapped cesium atoms at very high atomic densities, *Phys. Rev. Lett.* 81 (26) (1998) 5768–5771.
- [5] M. Morinaga, I. Bouchoule, J. C. Karam, C. Salomon, Manipulation of motional quantum states of neutral atoms, *Phys. Rev. Lett.* 83 (1999) 4037–4040.
- [6] J. Ringot, P. Szriftgiser, J. C. Garreau, D. Delande, Experimental evidence of dynamical localization and delocalization in a quasiperiodic driven system, *Phys. Rev. Lett.* 85 (13) (2000) 2741–2744.
- [7] D. A. Steck, W. H. Oskay, M. G. Raizen, Fluctuations and Decoherence in Chaos-Assisted Tunneling, *Phys. Rev. Lett.* 88 (12) (2002) 120406.
- [8] M. B. Dahan, E. Peik, J. Reichel, Y. Castin, C. Salomon, Bloch Oscillations of Atoms in an Optical Potential, *Phys. Rev. Lett.* 76 (24) (1996) 4508–4511.
- [9] Q. Niu, X. G. Zhao, G. A. Georgakis, M. G. Raizen, Atomic Landau-Zener Tunneling and Wannier-Stark Ladders in Optical Potentials, *Phys. Rev. Lett.* 76 (24) (1996) 4504 – 4507.
- [10] S. R. Wilkinson, C. F. Bharucha, K. W. Madison, Q. Niu, M. G. Raizen, Observation of atomic Wannier-Stark ladders in an accelerating optical potential, *Phys. Rev. Lett.* 76 (24) (1996) 4512–4515.
- [11] I. Dotsenko, W. Alt, S. Kuhr, D. Schrader, M. Müller, Y. Miroshnychenko, V. Gomer, A. Rauschenbeutel, D. Meschede, Application of electro-optically generated light fields for Raman spectroscopy of trapped cesium atoms, *App. Phys. B* 78 (6) (2004) 711–717.
- [12] D. S. Weiss, B. C. Young, S. Chu, Precision measurement of the photon recoil of an atom using atomic interferometry, *Phys. Rev. Lett.* 70 (18) (1993) 2706–2709.
- [13] R. Battesti, P. Cladé, S. Guellati-Khélifa, C. Schwob, B. Grémaud, F. Nez,

- L. Julien, F. Biraben, Bloch Oscillations of Ultracold Atoms: A Tool for a Metrological Determination of h/m_{Rb} , *Phys. Rev. Lett.* 92 (25) (2004) 253001.
- [14] P. Cladé, E. de Mirandes, M. Cadoret, S. Guellati-Khélifa, C. Schwob, F. Nez, L. Julien, F. Biraben, Determination of the Fine Structure Constant Based on Bloch Oscillations of Ultracold Atoms in a Vertical Optical Lattice, *Phys. Rev. Lett.* 96 (3) (2006) 033001.
- [15] K. Gibble, S. Chu, Laser-cooled Cs frequency standard and a measurement of the frequency shift due to ultracold collisions, *Phys. Rev. Lett.* 70 (12) (1993) 1771–1774.
- [16] K. L. Corwin, S. J. M. Kuppens, D. Cho, C. E. Wieman, Spin-polarized atoms in a circularly polarized optical dipole trap, *Phys. Rev. Lett.* 83 (1999) 1311–1314.
- [17] H. Perrin, A. Kuhn, I. Bouchoule, T. Pfau, C. Salomon, Raman cooling of spin-polarized cesium atoms in a crossed dipole trap, *Europhys. Lett.* 46 (2) (1999) 141–147.
- [18] D. J. Han, S. Wolf, S. Oliver, C. McCormick, M. T. Depue, D. S. Weiss, 3D Raman Sideband Cooling of Cesium Atoms at High Density, *Phys. Rev.* 85 (4) (2000) 724–727.
- [19] J. Ringot, P. Szriftgiser, J. C. Garreau, Subrecoil Raman spectroscopy of cold cesium atoms, *Phys. Rev. A* 65 (1) (2001) 013403.
- [20] C. Salomon, J. Dalibard, W. D. Phillips, A. Clairon, S. Guellatti, Laser Cooling of Cesium Atoms below $3 \mu\text{K}$, *Europhys. Lett.* 12 (8) (1990) 683–688.
- [21] J. Ringot, Y. Lecoq, J. C. Garreau, P. Szriftgiser, Generation of phase-coherent laser beams for Raman spectroscopy and cooling by direct current modulation of diode laser, *Eur. Phys. J. D* 7 (3) (1999) 285–288.
- [22] D. A. Steck, Quantum chaos, transport, and decoherence in atom optics, Ph.D. thesis, University of Texas, USA, Unpublished (2001).
- [23] G. Avila, V. Giordano, V. Candelier, E. de Clercq, G. Theobald, P. Cerez, State selection in a cesium beam by laser-diode optical pumping, *Phys. Rev. A* 36 (8) (1987) 3719–3728.
- [24] J. Sagle, R. K. Namiotka, J. Huennekens, Measurement and modelling of intensity dependent absorption and transit relaxation on the cesium D1 line, *J. Phys. B: At. Mol. Opt. Phys.* 29 (12) (1996) 2629–2643.